

# SpinGlassPEPS.jl: Tensor-network package for Ising-like optimization on quasi-two-dimensional graphs

Tomasz Śmierzchalski<sup>a</sup>, Anna M. Dziubyna<sup>b,c</sup>, Konrad Jałowiecki<sup>a</sup>, Zakaria Mzaouali<sup>a</sup>, Łukasz Paweła<sup>a</sup>, Bartłomiej Gardas<sup>a</sup>, Marek M. Rams<sup>b</sup>

<sup>a</sup>*Institute of Theoretical and Applied Informatics, Polish Academy of Sciences, Bałtycka 5, 44-100 Gliwice, Poland*

<sup>b</sup>*Jagiellonian University, Institute of Theoretical Physics, Łojasiewicza 11, 30-348 Kraków, Poland*

<sup>c</sup>*Jagiellonian University, Doctoral School of Exact and Natural Sciences, Łojasiewicza 11, 30-348, Kraków, Poland*

---

## Abstract

This work introduces `SpinGlassPEPS.jl`, a software package implemented in Julia, designed to find low-energy configurations of generalized Potts models, including Ising and QUBO problems, utilizing heuristic tensor network contraction algorithms on quasi-2D geometries. In particular, the package employs the Projected Entangled-Pairs States to approximate the Boltzmann distribution corresponding to the model's cost function. This enables an efficient branch-and-bound search (within the probability space) that exploits the locality of the underlying problem's topology. As a result, our software enables the discovery of low-energy configurations for problems on quasi-2D graphs, particularly those relevant to modern quantum annealing devices. The modular architecture of `SpinGlassPEPS.jl` supports various contraction schemes and hardware acceleration.

*Keywords:* spin-glass problems, tensor network contractions, QUBO, Ising model, Random Markov Field

---

## Required Metadata

Nr.	Code metadata description	Please fill in this column
C1	Current code version	v1.4.1
C2	Permanent link to code/repository used for this code version	<a href="https://github.com/euro-hpc-pl/SpinGlassPEPS.jl">https://github.com/euro-hpc-pl/SpinGlassPEPS.jl</a>
C4	Legal Code License	Apache 2.0
C5	Code versioning system used	git
C6	Software code languages, tools, and services used	Julia
C7	Compilation requirements, operating environments & dependencies	Julia 1.11, CUDA.jl v5, TensorOperations.jl, Memoize.jl
C8	If available, Link to developer documentation/manual	<a href="https://euro-hpc-pl.github.io/SpinGlassPEPS.jl/dev/">https://euro-hpc-pl.github.io/SpinGlassPEPS.jl/dev/</a>
C9	Support email for questions	lpawela@iitis.pl

Table 1: Code metadata

## 1. Motivation and significance

`SpinGlassPEPS.jl` provides a robust software package designed to find low-energy configurations for generalized Potts models [1], including Ising [2] or equivalently Quadratic Unconstrained Binary Optimization (QUBO) problems. By leveraging heuristic tensor network algorithms, specifically Projected Entangled-Pairs States (PEPS) [3, 4, 5, 6], the package enables efficient exploration of low-energy solutions within complex problem topologies. This capability is particularly significant in the context of current quantum and classical annealing devices [7, 8, 9], where efficient and scalable solutions are essential.

The significance of `SpinGlassPEPS.jl` lies in its ability to lower the entry barrier to applying advanced tensor network methods in classical optimization. It offers a modular architecture that supports various contraction schemes and hardware acceleration, making it adaptable to a wide range of problem instances. The software has been extensively benchmarked [10] on problems defined on D-Wave’s Pegasus and Zephyr geometries [11, 12].

## 2. Software description

`SpinGlassPEPS.jl` is a collection of Julia [13] packages implementing heuristic tensor-network based algorithm to find low-energy states and their

corresponding energies (i.e., the spectrum) of generalized Potts model,

$$E(\mathbf{x}) = \sum_{\langle m,n \rangle \in \mathcal{F}} E_{m,n}(x_m, x_n) + \sum_{n \in \mathcal{W}} E_n(x_n), \quad (1)$$

defined on a graph  $\mathcal{G} = (\mathcal{W}, \mathcal{F})$  specified by its edges,  $\mathcal{F}$ , and vertices,  $\mathcal{W}$ . The method tackles a family of sparse two-dimensional graphs called king's graphs [14], see Fig. 1(b). A particular problem instance is defined by real-valued functions,  $E_n(x_n)$  and  $E_{m,n}(x_m, x_n)$ , where  $n, m \in \mathcal{W}$ .

In particular, this includes the Ising model,

$$E(\mathbf{s}) = \sum_{\langle i,j \rangle \in \mathcal{E}} J_{ij} s_i s_j + \sum_{i \in \mathcal{V}} h_i s_i, \quad (2)$$

defined on  $\mathcal{G}' = (\mathcal{V}, \mathcal{E})$ , where  $i, j \in \mathcal{V}$ ,  $J_{ij}, h_i \in \mathbb{R}$  and  $s_i \in \{-1, 1\}$ . The Ising model can be considered a special case of the Potts model, and we extend this by allowing clusters of spin variables to be grouped into effective Potts degrees of freedom with higher dimensions. This approach enables the package to manage more complex quasi-2D graph geometries, including those relevant to current quantum and classical annealing device architectures.

The algorithm executes a branch-and-bound search [15] within the probability space defined by the Boltzmann distribution at a specific inverse temperature  $\beta$ . This search process involves constructing a predefined number of the most probable local configurations of Potts variables, progressing sequentially from one vertex to the next until the entire system has been explored. The emphasis on king's graphs is incorporated into the algorithm at two distinct levels.

First, in calculating marginal probabilities, we employ a tensor network representation of the classical Boltzmann distribution. For two-dimensional systems, this representation takes the form of PEPS. The marginal and conditional probabilities are derived from the contraction of the tensor network. Although the problem of contracting these networks is formally #P-hard [16], we utilize an established approximate (heuristic) framework to contract two-dimensional PEPS [5, 6].

Furthermore, we leverage the locality of interactions within the graph to expand the search space by merging partial trial configurations that are equivalent in terms of the marginal conditional probabilities considered by the algorithm. Specifically, partial configurations with identical values of Potts variables on the boundary adjacent to unexplored regions of the graph are combined. This approach also enables the identification of information regarding local excitations in the system. When two partial configurations share boundary variables, they have a well-defined energy associated with the

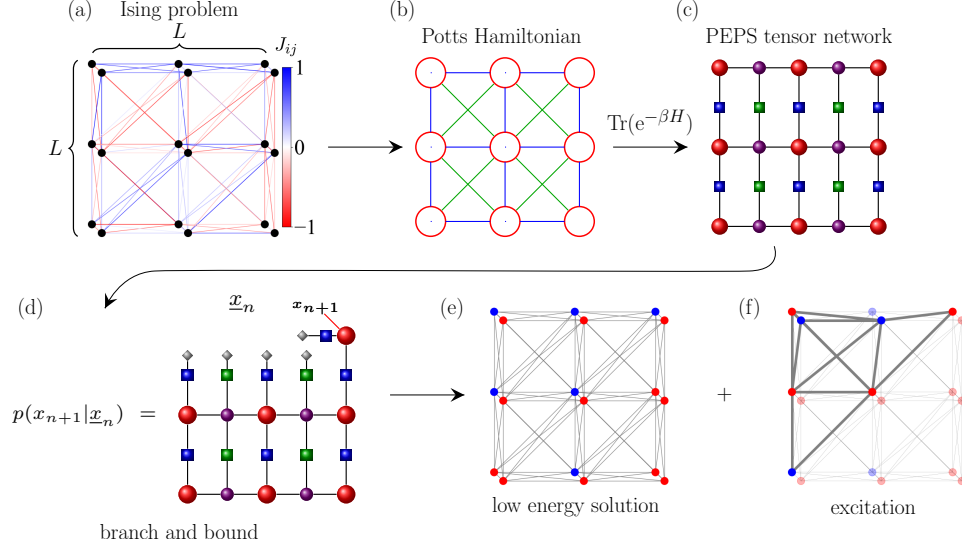


Figure 1: Execution flow. The Ising problem in (a) is mapped to a Potts Hamiltonian defined on a king's graph in (b). This allows the partition function of that Hamiltonian to be represented as a PEPS tensor network on a square lattice, as in (c). The main algorithm executes the branch and bound search in the probability space, building the most probable configurations by adding one Potts variable at a time. The marginal conditional probabilities follow from an approximate contraction of the corresponding tensor network in (d). The full branch and bound sweep results in a candidate for the most probable (ground state) configuration in (e), together with a set of localized excitations on top of it in (f).

bulk variables, where one configuration represents a local ground state and the other an excitation localized in the bulk. By collecting such information throughout the search, the algorithm generates a candidate for the ground state along with a set of excited low-energy states, effectively characterizing the low-energy manifold of the optimization problem.

The algorithm workflow is outlined in Fig. 1. The package is designed with a modular architecture that captures the relationships between the high-level concepts employed by the algorithm. This modularity enables the integration of various contraction schemes, leveraging the internal structures of individual tensors within the network, and allows for hardware acceleration, all facilitated by the multiple dispatch capabilities of the Julia language. Detailed explanations of the algorithm's mechanics, along with extensive benchmarks for Pegasus and Zephyr geometries, relevant for D-Wave quantum annealers, are provided in [10].

### 2.1. Software Architecture

`SpinGlassPEPS.jl` is composed of three independent sub-packages, each of which is responsible for distinct elements of the workflow, see Fig. 2. Namely,

- `SpinGlassEngine.jl` serves as the core package, consisting of routines for executing the branch-and-bound method (with the ability to leverage the problem’s locality) for a given Potts instance. It also includes capabilities for reconstructing the low-energy spectrum from identified localized excitations and provides a tensor network constructor.
- `SpinGlassNetworks.jl` facilitates the generation of an Ising graph from a given instance using a set of standard inputs (e.g., instances compatible with the Ocean environment provided by D-Wave) and supports clustering to create effective Potts Hamiltonians.
- `SpinGlassTensors.jl` offers essential tools to create and manipulate tensors that build the PEPS network, with support for CPU and GPU utilization. It manages core operations on tensor networks, including contraction, using the boundary Matrix Product State approach [5]. This package primarily functions as a backend and users generally do not interact with it directly.

The `SpinGlassPEPS.jl` can be installed using the Julia package manager for Julia v1.11. In Julia REPL type `]` to enter `Pkg REPL`, then type:

```
pkg> add SpinGlassPEPS
```

### 2.2. Software Functionalities

For Ising/QUBO problems, the package requires instances to be provided in a specific format, similar to the one used in Stanford Gset (reduced from Max-Cut) [17]. In this format, the spins are numbered 1 to  $N$  and arranged in rows as  $i\ j\ v$ , where  $v$  represents the coupling value between vertices  $i$  and  $j$ , or the local magnetic field when  $i = j$ .

The algorithm produces a low-energy spectrum as its output, detailing the states and their corresponding energies for the given input instance. In addition, the package provides supplementary information, such as the estimated probabilities of these states derived from the approximate contraction of the tensor network.

The package’s modular structure offers a range of options to control various aspects of the main algorithm. These include the details and control

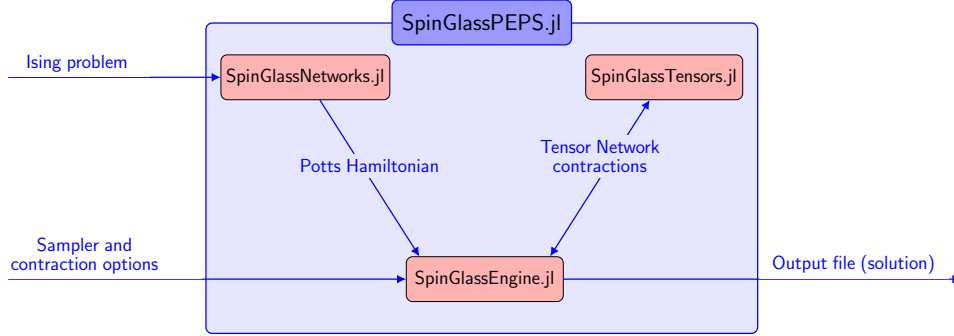


Figure 2: Interoperability between all `SpinGlassPEPS.jl` packages. The input Ising problem file is processed by `SpinGlassNetworks.jl`, transforming it into a Potts Hamiltonian. The latter is then passed to `SpinGlassEngine.jl`, together with solver’s and contraction’s parameters. The `SpinGlassEngine.jl` module serves as the core branch and bound solver. It passes the problem of marginal probabilities’ calculation to `SpinGlassTensors.jl`, that constructs and approximately contracts the corresponding tensor network. Finally, the solution (ground state, excitations, and their energies) is returned to the user as an output.

parameters of the tensor network contraction schemes, the ability to utilize either CPU or GPU for low-level operations, and the choice between constructing the tensor network in a dense or sparse format. The sparse format leverages the internal structures of individual tensors and is particularly essential for handling large clusters, such as those relevant to Pegasus and Zephyr graphs. Detailed information on all required and optional parameters is available in the documentation [18].

### 3. Illustrative Examples

We illustrate the capabilities and modularity of `SpinGlassPEPS.jl` by addressing two distinct problems. First, we solve an Ising problem defined on a quasi-2D graph, see Fig. 1(a). Although this example focuses on a specific topology, the approach is applicable to other structures, including those used in D-Wave systems. The second example tackles an inpainting problem formulated through the Potts model [19, 20, 21].

The code for all the examples presented below can be found in the main repository [22] folder “examples”. To run them, first, clone the repository. Then, run Julia inside the “examples” folder. The environment needed to execute the provided code is given by the `Project.toml` file. It can be activated by typing `]` in Julia REPL and then:

```
pkg> activate .
pkg> instantiate
```

next in Julia REPL type:

```
julia> include("ising_model_on_a_kings_graph.jl")
```

Alternatively, one can run the examples by typing:

```
$ julia --project=. -e "using Pkg; Pkg.instantiate()"
```

```
$ julia --project=. ising_model_on_a_kings_graph.jl
```

in the preferred shell.

While the Ising model on a king's graph should compute relatively fast, the latter two examples (an inpainting example and a small pegasus-type graph) can take a long time to finish if run on the CPU only. It is recommended to run them using GPU.

### 3.1. Ising model on a king's graph

In the listing below, we show a complete Julia script to define and solve an Ising problem defined on a graph in Fig. 1(a).

```
using SpinGlassPEPS

function get_instance(topology::NTuple{3, Int})
    m, n, t = topology
    "$(@__DIR__)/instances/$(m)x$(n)x$(t).txt"
end

function run_square_diag_bench(::Type{T}; topology::NTuple{3, Int}) where {T}
    m, n, _ = topology
    instance = get_instance(topology)
    lattice = super_square_lattice(topology)

    hamming_dist = 5
    eng = 10

    best_energies = T[]

    potts_h = potts_hamiltonian(
        ising_graph(instance),
        spectrum = full_spectrum,
        cluster_assignment_rule = lattice,
    )
```

```

params = MpsParameters{T} (; bond_dim = 16, num_sweeps = 1)
search_params = SearchParameters (; max_states = 2^8, cut_off_prob = 1E-4)

for transform ∈ all_lattice_transformations
    net = PEPSNetwork{KingSingleNode{GaugesEnergy}, Dense, T}(
        m, n, potts_h, transform,
    )

    ctr = MpsContractor(SVDTruncate, net, params;
        onGPU = false, beta = T(2), graduate_truncation = true,
    )

    single = SingleLayerDroplets(eng, hamming_dist, :hamming)
    merge_strategy = merge_branches(
        ctr; merge_type = :nofit, update_droplets = single,
    )

    sol, _ = low_energy_spectrum(ctr, search_params, merge_strategy)

    push!(best_energies, sol.energies[1])
    clear_memoize_cache()
end

ground = best_energies[1]
@assert all(ground .≈ best_energies)

println("Best energy found: $(ground)")
end

T = Float64
@time run_square_diag_bench(T; topology = (3, 3, 2))

```

In the example above, `transform` specifies a rotation of the quasi-2D graph. The branch-and-bound search operates with a fixed order of sweeping through local variables, corresponding to the fixed order of tensor network contraction. By rotating the network, the search and contraction can effectively begin from different starting points on the 2D grid, thereby enhancing the stability of the results. This example performs the search across all eight possible transformations of the 2D grid, comparing the best energies obtained for each configuration.

Other control parameters include `Sparsity`, which determines whether dense or sparse tensors should be used. The concept of sparse tensors was introduced to manage large clusters containing  $\mathcal{O}(10\text{--}20)$  Ising variables



(*i.e.*, spins) each, where explicit construction of PEPS tensors, triggered by `Sparsity=Dense`, quickly becomes infeasible. Conversely, `Sparsity=Sparse` circumvents the need for direct construction of individual tensors by performing optimal contractions on small tensor diagrams utilizing internal structure of individual tensors. These diagrams are then combined to efficiently contract the entire network. Finally, `Node = KingSingleNode{GaugesEnergy}` specifies the type of the node used within the tensor networks (e.g., switching between king’s graph or a square lattice); `Layout = GaugesEnergy` denotes the division of the PEPS network into boundary Matrix Product States [5, 6] used to contract the network.

Low-energy excitations (*i.e.*, droplets) above the best solution can be identified during the optional `merge_branches` step. This option can be provided as an argument to the function that executes the branch-and-bound algorithm, `low_energy_spectrum` (see [10] for extended discussion). To view all droplets found, one may invoke `unpack_droplets(solution)`.

The algorithm searches for diverse excitations within a specified energy range above the ground state. An excitation is accepted only if its Hamming distance from any previously identified excitation exceeds a predefined threshold. This is governed by the parameters `energy_cutoff`, which sets the maximum allowed energy above the ground state, and `hamming_cutoff`, which determines the minimum Hamming distance required between excitations for them to be considered distinct.

We present a selected set of benchmark results in Fig. 3, focusing on two problem sets with 2500 and 5000 spins (a  $50 \times 50$  grid with 1 and 2 spins per cluster, respectively). The reference results are compared against those obtained from Simulated Bifurcation Machine (SBM) [8] and CPLEX solvers [23].

For an instances with 2500 spins, `SpinGlassPEPS.jl` successfully found the ground states for all cases, as certified by CPLEX, outperforming SBM in these tests. This demonstrates that, in certain scenarios (e.g., king’s graph), our approach can exceed state-of-the-art methods. For 5000 spins, SBM delivers the best results; however, `SpinGlassPEPS.jl` still performs better than CPLEX, which faces challenges with larger problem sizes.

Both `SpinGlassPEPS.jl` and SBM can output multiple solutions (*i.e.*, low-energy states), whereas CPLEX generates only one. When considering time to solution, our method is typically the most time-intensive, while SBM is the fastest across all tested solvers since it can be GPU-accelerated efficiently.

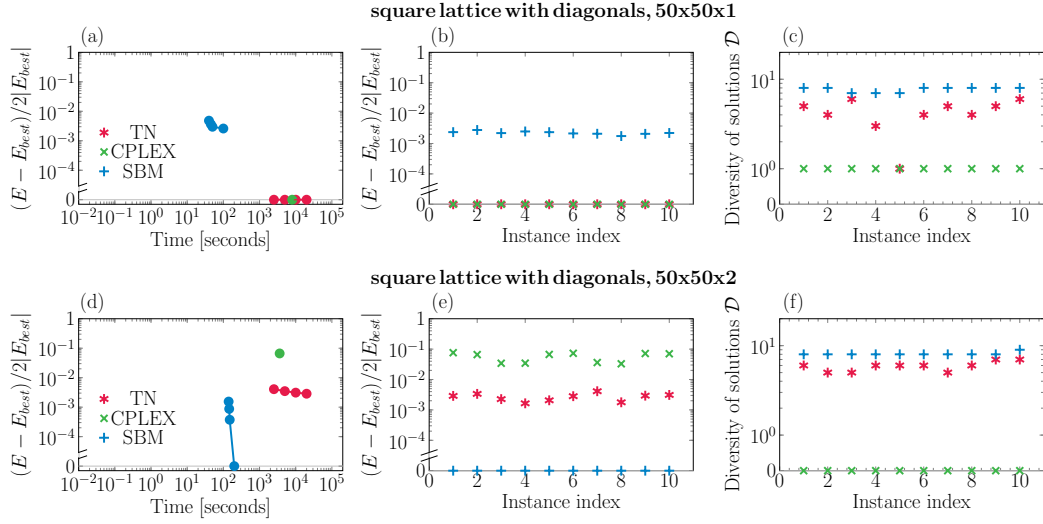


Figure 3: Benchmarking `SpinGlassPEPS.jl` for two sets of Ising problems defined on graphs from Fig. 1(a) with  $N = 50 \times 50 \times d$  spins, for  $d = 1$  (top row) and  $d = 2$  (bottom row). As reference solvers, We employ a Simulated Bifurcation machine (SBM) [24] and CPLEX. Panels (a) and (d) show time to solution to the best energy for a median instance ( $E_{\text{best}}$  is the best results among the considered solvers), and in (b) and (e), we show instance-wise results for 10 instances. In (c) and (f), we show the diversity of obtained solutions, *i.e.*, the number of solutions within approximation ratio  $a_r = 0.01$  ( $E - E_{\text{best}} < a_r \cdot 2 \cdot E_{\text{best}}$ ), where each pair has a Hamming distance greater than  $N/2$ .

### 3.1.1. Large unit cells

Our package can target the graphs that can be manufactured by quantum annealing vendors (cf., D-Wave processors depicted in Fig. 4). We provide an extensive benchmark of our approach for those geometries elsewhere [10].

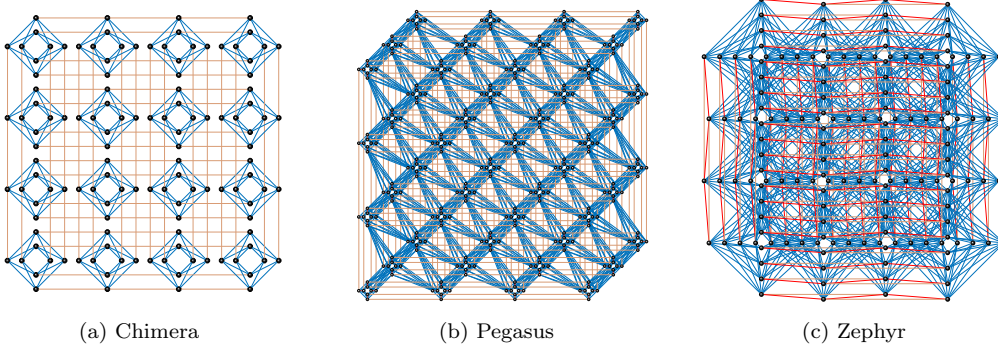


Figure 4: Problems defined on Chimera, Pegasus, and Zephyr graphs [11, 25, 12, 26], employed in the past and current D-Wave quantum annealers, can be mapped to the Potts Hamiltonian on king’s graph upon grouping 8, 24, and 16 spins, respectively. Due to the large unit cell size of the latter two graphs, they require further processing. In particular, sparse connectivity structures between unit cells and GPU acceleration. Both are supported by `SpinGlassPEPS.jl` package.

### 3.2. Solving Potts model - inpainting problem

The Potts model defined in Eq. (1) is general enough to describe a wide array of phenomena. One of them is the problem of inpainting in computer vision. It refers to filling in missing or corrupted parts of an image in a way that makes the reconstruction visually plausible [27]. In this example, we use a relatively small benchmarking instance given by [19, 21]. It is a discretized triple junction inpainting problem, as shown in Fig. 5. The software accepts instances formatted as in OpenGM Benchmark dataset [21] with only the nearest neighbor and diagonal interactions.

```
instance = "$(@__DIR__)/instances/triplepoint4-plain-ring.h5"
# We add size of picture in pixels
potts_h = potts_hamiltonian(instance, 120, 120)
```

In this case, when searching for droplets, one should set `mode` parameter in `SingleLayerDroplets` to `:RMF`.

```
droplets = SingleLayerDroplets(; max_energy = 100, min_size = 100,
    metric = :hamming, mode=:RMF)
```

The remaining setup is analogous to the king’s graph scenario described in the preceding section.



Figure 5: The picture in panel (a) shows the used inpainting problem. Data is given on the circular boundary, and the solution should fill in the black region. It is part of the OpenGM2 Benchmark dataset [21]. The picture in panel (b) shows the ground state obtained by `SpinGlassPEPS.jl`. Due to the introduced anisotropy by the grid used in discretization, the results show a bias toward axis-parallel edges [19]. Yellow region in (c) shows a low-energy excitation, *i.e.*, a group of variables that should be collectively filled to obtain another low-energy solution.

#### 4. Impact and Conclusion

Tensor networks offer a powerful suite of tools, most notably employed in quantum many-body simulations. Our package reduces the hurdles for applying these methods to classical optimization [28]. Building on the framework introduced in Ref. [29] – originally targeting simpler Chimera-like graphs – `SpinGlassPEPS.jl` provides a flexible software platform for a broader range of problem topologies, utilizing sparse tensor structures, efficient use of GPU, etc.

As such, `SpinGlassPEPS.jl` acts as a practical reference tool to develop and work with quantum and classical annealing technologies. The examples presented show that the tensor network approach can achieve high-quality solutions comparable to those of CPLEX, a state-of-the-art solver in operational research [23]. Notably, for certain king’s graphs [14], our solutions surpass those from Toshiba’s Simulated Bifurcation Machines (SBM [8]), which is an unexpected result that merits further investigation. This highlights a potential weakness in the SBM family of algorithms, demonstrating the practical value of our software.

#### Acknowledgments

This project was supported by the National Science Center (NCN), Poland, under Projects: Sonata Bis 10, No. 2020/38/E/ST3/00269 (T.S., Z.M.) and 2020/38/E/ST3/00150 (A.D., M.R.) and Foundation for Polish Science

(grant no POIR.04.04.00-00-14DE/ 18-00 carried out within the Team-Net program co-financed by the European Union under the European Regional Development Fund) (B.G., L.P.).

## References

- [1] W. Kinzel, E. Domany, Critical properties of random Potts models, *Physical Review B* 23 (1981) 3421–3434. [doi:10.1103/PHYSREVB.23.3421](https://doi.org/10.1103/PHYSREVB.23.3421).
- [2] A. Lucas, Ising formulations of many NP problems, *Frontiers in Physics* 2 (5) (2014). [doi:10.3389/fphy.2014.00005](https://doi.org/10.3389/fphy.2014.00005).
- [3] T. Nishino, Y. Hieida, K. Okunishi, N. Maeshima, Y. Akutsu, A. Gen-diar, Two-dimensional tensor product variational formulation, *Progress of Theoretical Physics* 105 (3) (2001) 409–417. [doi:10.1143/PTP.105.409](https://doi.org/10.1143/PTP.105.409).
- [4] F. Verstraete, M. M. Wolf, D. Perez-Garcia, J. I. Cirac, Criticality, the area law, and the computational power of projected entangled pair states, *Physical Review Letters* 96 (22) (2006) 220601. [doi:10.1103/PhysRevLett.96.220601](https://doi.org/10.1103/PhysRevLett.96.220601).
- [5] F. Verstraete, J. I. Cirac, V. Murg, Matrix Product States, Projected Entangled Pair States, and variational renormalization group methods for quantum spin systems, *Advances in Physics* 57 (2) (2008) 143–224. [doi:10.1080/14789940801912366](https://doi.org/10.1080/14789940801912366).
- [6] R. Orús, A practical introduction to tensor networks: Matrix product states and projected entangled pair states, *Annals of Physics* 349 (2014) 117–158. [doi:https://doi.org/10.1016/j.aop.2014.06.013](https://doi.org/10.1016/j.aop.2014.06.013).
- [7] A. D. King, et al., Quantum critical dynamics in a 5,000-qubit programmable spin glass, *Nature* 617 (7959) (2023) 61–66. [doi:10.1038/s41586-023-05867-2](https://doi.org/10.1038/s41586-023-05867-2).
- [8] H. Goto, K. Endo, M. Suzuki, Y. Sakai, T. Kanao, Y. Hamakawa, R. Hidaka, M. Yamasaki, K. Tatsumura, High-performance combinatorial optimization based on classical mechanics, *Science Advances* 7 (6) (2021) eabe7953. [doi:10.1126/sciadv.abe7953](https://doi.org/10.1126/sciadv.abe7953).
- [9] J. Wang, D. Ebler, K. Y. M. Wong, D. S. W. Hui, J. Sun, Bifurcation behaviors shape how continuous physical dynamics solves discrete Ising optimization, *Nature Communications* 14 (1) (2023) 2510. [doi:10.1038/s41467-023-37695-3](https://doi.org/10.1038/s41467-023-37695-3).

- [10] A. M. Dziubyna, T. Śmierzchalski, B. Gardas, M. M. Rams, M. Mohseni, Limitations of tensor network approaches for optimization and sampling: A comparison against quantum and classical Ising machines, arXiv:2411.16431 (2024). doi:10.48550/arXiv.2411.16431.
- [11] K. Boothby, D. King, Andrew, J. Raymond, Zephyr Topology of D-Wave Quantum Processors, Tech. Rep. 14-1056A-A, D-Wave, [https://www.dwavesys.com/media/2uznec4s/14-1056a-a\\_zephyr\\_topology\\_of\\_d-wave\\_quantum\\_processors.pdf](https://www.dwavesys.com/media/2uznec4s/14-1056a-a_zephyr_topology_of_d-wave_quantum_processors.pdf) [accessed 31 January 2024] (2021).
- [12] N. Dattani, S. Szalay, N. Chancellor, Pegasus: The second connectivity graph for large-scale quantum annealing hardware, arXiv:1901.07636 (2019). doi:10.48550/arXiv.1901.07636.
- [13] J. Bezanson, A. Edelman, S. Karpinski, V. B. Shah, Julia: A fresh approach to numerical computing, SIAM Review 59 (1) (2017) 65–98. doi:10.1137/141000671.
- [14] G. J. Chang, Algorithmic aspects of domination in graphs, in: P. M. Pardalos, D.-Z. Du, R. L. Graham (Eds.), Handbook of Combinatorial Optimization, Springer New York, New York, NY, 2013, pp. 221–282. doi:10.1007/978-1-4419-7997-1\_26.
- [15] D. R. Morrison, S. H. Jacobson, J. J. Sauppe, E. C. Sewell, Branch-and-bound algorithms: A survey of recent advances in searching, branching, and pruning, Discrete Optimization 19 (2016) 79–102. doi:https://doi.org/10.1016/j.disopt.2016.01.005.
- [16] N. Schuch, M. M. Wolf, F. Verstraete, J. I. Cirac, Computational complexity of Projected Entangled Pair States, Physical Review Letters 98 (14) (2007) 140506. doi:10.1103/PhysRevLett.98.140506.
- [17] Stanford University, Index of /~yyye/yyye/gset, <https://web.stanford.edu/~yyye/yyye/Gset/>, [accessed 19 May 2024] (2003).
- [18] T. Śmiechrzalski, A. M. Dziubyna, Ł. Pawela, B. Gardas, M. M. Rams, Spinglasspeps.jl documentation, <https://euro-hpc-pl.github.io/SpinGlassPEPS.jl>, [accessed 30 Jan 2025].
- [19] J. Lellmann, C. Schnörr, Continuous multiclass labeling approaches and algorithms, SIAM Journal on Imaging Sciences 4 (4) (2011) 1049–1096. doi:10.1137/100805844.

- [20] J. H. Kappes, M. Speth, G. Reinelt, C. Schnörr, Towards efficient and exact map-inference for large scale discrete computer vision problems via combinatorial optimization, in: 2013 IEEE Conference on Computer Vision and Pattern Recognition, 2013, pp. 1752–1758. doi:[10.1109/CVPR.2013.229](https://doi.org/10.1109/CVPR.2013.229).
- [21] J. H. Kappes, B. Andres, F. A. Hamprecht, C. Schnörr, S. Nowozin, D. Batra, S. Kim, B. X. Kausler, T. Kröger, J. Lellmann, N. Komodakis, B. Savchynskyy, C. Rother, A comparative study of modern inference techniques for structured discrete energy minimization problems, *International Journal of Computer Vision* (2015) 1–30. doi:[10.1007/s11263-015-0809-x](https://doi.org/10.1007/s11263-015-0809-x).
- [22] T. Śmiechrzalski, A. M. Dziubyna, L. Pawela, B. Gardas, M. M. Rams, Spinglasspeps.jl documentation, <https://github.com/euro-hpc-pl/SpinGlassPEPS.jl>, [accessed 30 Jan 2025]. doi:[10.5281/zenodo.14627392](https://doi.org/10.5281/zenodo.14627392).
- [23] CPLEX, IBM ILOG, *Users manual for cplex* (2024).  
URL <https://www.ibm.com/docs/en/icos/22.1.1?topic=optimizers-users-manual-cplex>
- [24] H. Goto, K. Tatsumura, A. R. Dixon, Combinatorial optimization by simulating adiabatic bifurcations in nonlinear Hamiltonian systems, *Science Advances* 5 (4) (2019) eaav2372. doi:[10.1126/sciadv.aav2372](https://doi.org/10.1126/sciadv.aav2372).
- [25] K. Boothby, P. Bunyk, J. Raymond, A. Roy, Next-generation topology of D-Wave quantum processors, Tech. Rep. 14-1026A-C, D-Wave, <https://www.dwavesys.com/media/jwwj5z3z/14-1026a-c-next-generation-topology-of-dw-quantum-processors.pdf> [accessed 31 January 2024] (2019).
- [26] T. Lanting, et al., Entanglement in a quantum annealing processor, *Physical Review X* 4 (2) (2014) 021041. doi:[10.1103/PhysRevX.4.021041](https://doi.org/10.1103/PhysRevX.4.021041).
- [27] Y. Zeng, Z. Lin, J. Yang, J. Zhang, E. Shechtman, H. Lu, High-resolution image inpainting with iterative confidence feedback and guided upsampling, in: A. Vedaldi, H. Bischof, T. Brox, J.-M. Frahm (Eds.), *Computer Vision – ECCV 2020*, Springer International Publishing, Cham, 2020, pp. 1–17. doi:[10.1007/978-3-030-58529-7\\_1](https://doi.org/10.1007/978-3-030-58529-7_1).

- [28] A. Cichocki, Tensor networks for big data analytics and large-scale optimization problems (2014). [arXiv:1407.3124](#), [doi:10.48550/arXiv.1407.3124](#).
- [29] M. M. Rams, M. Mohseni, D. Eppens, K. Jałowiecki, B. Gardas, Approximate optimization, sampling, and spin-glass droplet discovery with tensor networks, Physical Review E 104 (2) (2021) 025308. [doi:10.1103/PhysRevE.104.025308](#).